Elasticity of self-organized frustrated disordered spring networks

Tommaso Pettinari,[1,2,*] Gustavo During,[3,†] and Edan Lerner[1,‡]
[1]*Institute of Theoretical Physics, University of Amsterdam, Science Park 904, 1098 XH Amsterdam, the Netherlands*
[2]*Van der Waals-Zeeman Institute, University of Amsterdam, Science Park 904, 1098 XH Amsterdam, the Netherlands*
[3]*Instituto de Física, Pontificia Universidad Católica de Chile, 8331150 Santiago, Chile*

(Received 22 January 2024; accepted 23 April 2024; published 24 May 2024)

There have been some interesting recent advances in understanding the notion of mechanical disorder in structural glasses and the statistical mechanics of these systems' low-energy excitations. Here we contribute to these advances by studying a minimal model for structural glasses' elasticity in which the degree of mechanical disorder—as characterized by recently introduced dimensionless quantifiers—is readily tunable over a very large range. We comprehensively investigate a number of scaling laws observed for various macro, meso and microscopic elastic properties, and rationalize them using scaling arguments. Interestingly, we demonstrate that the model features the universal quartic glassy vibrational density of states as seen in many atomistic and molecular models of structural glasses formed by cooling a melt. The emergence of this universal glassy spectrum highlights the role of self-organization (toward mechanical equilibrium) in its formation, and elucidates why models featuring structural frustration alone do not feature the same universal glassy spectrum. Finally, we discuss relations to existing work in the context of strain stiffening of elastic networks and of low-energy excitations in structural glasses, in addition to future research directions.

DOI: 10.1103/PhysRevE.109.054906

I. INTRODUCTION

Many static and dynamic mechanical properties of structural glasses depend upon their featured degree of mechanical disorder. Some well-known examples manifesting this dependence include wave attenuation rates [1–6], elastoplastic responses [7–10], and fracture mechanics [11–13]. Consequently, many efforts attempting to identify useful and broadly applicable quantifiers of mechanical disorder in structural glasses were put forward in recent years [14–18]. These efforts complement a different class of approaches—applied predominantly to understanding the structure-dynamics relations in supercooled liquids (see e.g. [19,20])—in which glassy disorder is quantified via positional disorder (of the relevant constituents) alone, with little or no reference to mechanics. The role of disorder in the physics of glassy solids has been incorporated in various theoretical frameworks, e.g., the shear transformation zones theory [21] and heterogeneous elasticity theory [1,2].

One key challenge toward a thorough understanding of the elasticity of structural glasses involves identifying simple models or glass-formation protocols (or both) that allow workers to tune the degree of mechanical disorder of the model systems over a large range. This has been previously accomplished in Refs. [22,23] by allowing for additional degrees of freedom in the Hamiltonian of a generic glass forming model—in this case, the particles' effective sizes—, and subsequently freezing those additional degrees of freedom after glass formation. Computer glasses formed with this protocol showed remarkable stress-strain curves with very pronounced stress overshoots, which are reminiscent of those seen upon shear deformation of ultrastable glasses [9,10]. They also feature an enormous variability of the width-to-mean ratio of the sample-to-sample distribution of the shear modulus—denoted there, here, and in what follows as χ—, shown to vary by over a factor of four by tuning the stiffness associated with the additional degrees of freedom. This approach to tuning mechanical disorder in computer glasses was also employed in Ref. [13] where the said variability gives rise to a ductile-to-brittle transition in glassy samples under uniaxial tension.

Another route toward tuning mechanical disorder in simple models was put forward in Refs. [5,16,24,27,28]; there, the internal stresses of a conventional computer glass were artificially reduced, leading to smaller mechanical fluctuations in glassy samples. References [5,16] showed that this reduction of internal stresses can give rise to almost an order of magnitude variability of the mechanical-disorder quantifier χ. Using this approach, in Ref. [5] it was shown that attenuation rates of shear waves scales as χ^2, in agreement with the predictions of heterogeneous elasticity theory [1,2].

While the aforementioned exercises and protocols are undoubtedly useful and insightful, they produce glassy structures that cannot represent well the class of configurations obtained by cooling a liquid into a glass. In particular, glasses formed by quenching a liquid have been shown to feature a universal gapless nonphononic spectra $\mathcal{D}(\omega) \sim \omega^4$ [29–31] (here ω is an angular frequency), independent of glass formation history [32–34], spatial dimension [35], or any microscopic details [36]. In contrast, glassy structures formed with the aforementioned protocols—either by adding degrees of freedom during glass formation [22,23], or by

*t.pettinari@uva.nl
†gduring@fis.puc.cl
‡Corresponding author: e.lerner@uva.nl

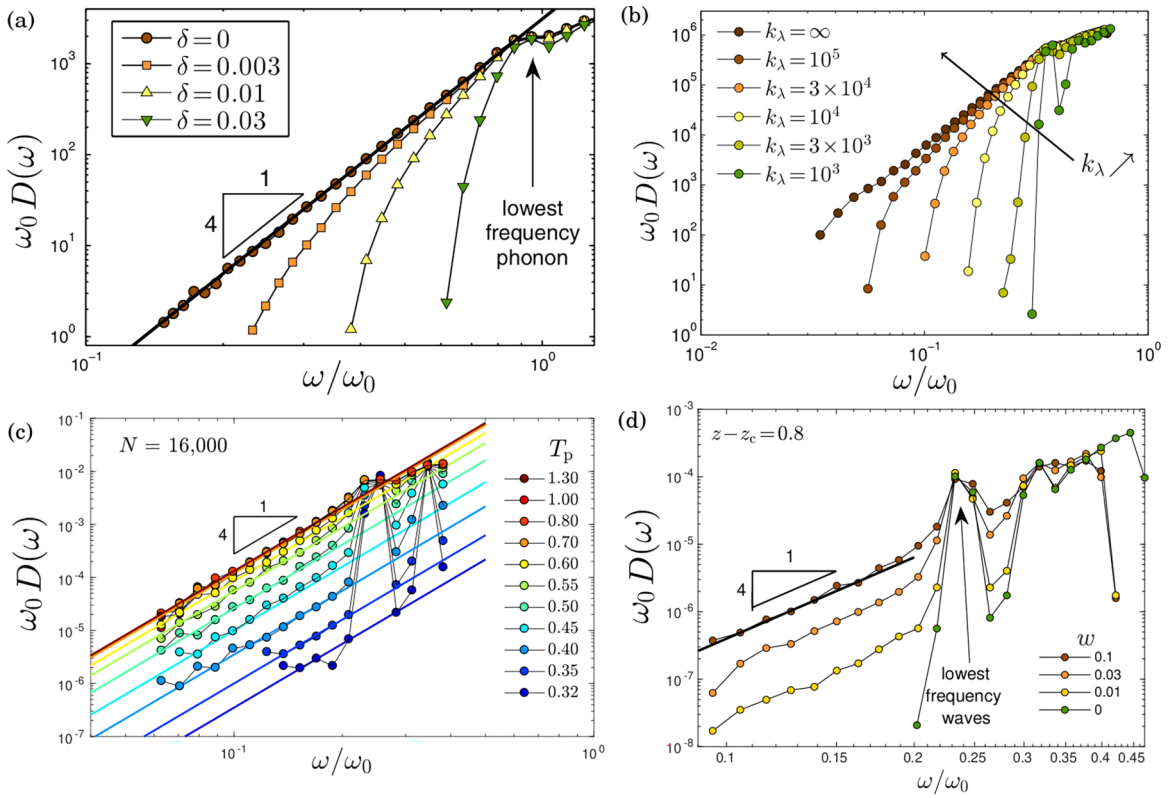

FIG. 1. (a) The vibrational density of states (VDoS) calculated for computer glasses in which the interparticle forces were factored by $1-\delta$, see legend for values of δ. Setting $\delta > 0$ results in a gap $\sim\sqrt{\delta}$ in the VDoS [24]. Here and in (b)–(d), $\omega_0 \equiv c_s/a_0$ where c_s is the speed of shear waves and a_0 an interparticle length. Figure adopted from Ref. [24]. (b) VDoS of computer glasses in which the particles' effective sizes are allowed to vary under a potential of characteristic stiffness k_λ only during glass formation (and frozen thereafter). A gap $\sim 1/\sqrt{k_\lambda}$ opens in the VDoS. Figure adopted from Ref. [23]. These two examples demonstrate that some approaches to tuning mechanical disorder in computer glasses result in anomalous vibrational spectra compared to those of glasses quenched from a melt–which universally feature $\sim\omega^4$ nonphononic spectra, as shown in panel (c) for glasses made with the Swap-Monte Carlo method introduced in Ref. [25]. Figure adopted from Ref. [26]. In this work we present a model and sample-formation protocol that both allows for a large tunability of mechanical disorder, and features the universal quartic nonphononic spectrum as shown in panel (d) and discussed in Sec. IV below.

artificially reducing the internal stresses [5,16,24,27,28]—feature a gapped nonphononic spectra (see examples in Fig. 1), rendering them less realistic and thus less relevant to natural or laboratory glasses.

In this work we study a minimal off-lattice model system and glass-formation protocol that—when employed together—allow for a very large tunability of mechanical disorder, while also featuring the universal $\sim\omega^4$ nonphononic spectrum as seen in computer glasses formed by quenching a melt, see Fig. 1 and associated caption. We study various micro, meso, and macroscopic observables as a function of the model's key parameters, and rationalize the observed scaling laws using scaling ansatz and arguments. We further discuss the relation of our work to a recently introduced class of mean-field models for glassy excitations [37,38], to the phenomenon of strain stiffening of elastic networks [39–41], and to other recent relevant work. Finally, future research directions are proposed.

II. MODEL AND SAMPLE-FORMATION PROTOCOL

We consider a minimal model consisting of a disordered Hookean-spring network in three dimensions (3D), connected at each of its N nodes to pointlike unit masses. The networks analyzed are constructed by adopting the contact network between particles of well-compressed packings of soft (harmonic) spheres. The edges of the adopted network are pruned to reach some target mean coordination z; in order to avoid dangling nodes or other unusual structural fluctuations, the pruning is done following the scheme described in Ref. [42] that reduces node-to-node coordination fluctuations. In this edge-pruned initial spring network, all of the springs' restlengths are set to be equal to those springs' actual lengths, and so there is initially no energy, stresses, nor frustration in the network. The springs all share the same stiffness k, set to unity in what follows. We use $a_0 \equiv (V/N)^{1/d}$ as the units of length (set to unity), such that, in what follows, energies are expressed in terms of ka_0^2, and stresses, pressures, and elastic moduli in terms of k/a_0.

In the next step of constructing glassy samples from our simple model, we introduce shifts $\delta\ell_{ij}$ in the restlengths ℓ_{ij} of the springs. The restlength-shifts $\delta\ell_{ij}$ are drawn from a Gaussian distribution with zero mean and width w; the latter forms one of the two key parameters of this model system (along with the coordination z). The introduction of shifts in the springs' restlengths leads to mechanical imbalance, which

is then eliminated by a potential-energy minimization [43], during which the system self-organizes into a state satisfying mechanical equilibrium. To avoid finite-size effects, we used the scheme described above to construct mechanically frustrated networks with $N=62\,500$ nodes; unless stated otherwise, the data below is reported for this system size. Finally, the averaging of all the observables of interest was performed over a set of 500 independently built networks (again, unless explicitly stated otherwise).

The model and glass-formation protocol described above are identical to one of the three variants put forward very recently in [44]; in that work the focus is on the floppy regime $z<z_c=2\bar{d}$ with $\bar{d}$ denoting the dimension of space. Our model and protocol also bear similarity to the protocol and glass former employed in Ref. [6] to create glassy configurations over a wide range of mechanical disorder, which also features the universal $\sim\omega^4$ nonphononic spectrum. We discuss our results in the context of these prior works in the discussion section.

III. RESULTS

A. Notation and formalism

Before presenting our numerical results, we briefly review some of the formalism used to rationalize our observations. In particular, we adopt the bra-ket notation of Refs. [45,46] and make use of the equilibrium matrix $\mathcal{S}^T$ [47] that takes the vector sum of pairwise (spring) forces $|f\rangle$ exerted on each node, and results in a vector $|F\rangle$ of the net force on those nodes, namely,

$$|F\rangle = \mathcal{S}^T|f\rangle. \tag{1}$$

Furthermore, we make use of the known form of the nonphononic vibrational density of states $\mathcal{D}(\omega)$ in relaxed spring networks at some coordination z, namely, that a plateau of extended anomalous vibrational modes emerges from a frequency $\omega_\star\sim z-z_c\equiv\delta z$ [48–51].

Finally, denoting the potential energy by $U(\boldsymbol{x})$ and coordinates by $\boldsymbol{x}$, we use that the Hessian matrix $\boldsymbol{\mathcal{H}}\equiv\frac{\partial^2 U}{\partial\boldsymbol{x}\partial\boldsymbol{x}}$ of a relaxed spring network (of springs of unit stiffness, as in our model) reads [45]

$$\mathcal{H}=\mathcal{S}^T\mathcal{S}. \tag{2}$$

Furthermore, the eigenvectors $|\Psi_l\rangle$ of $\mathcal{H}$ satisfy [45]

$$\mathcal{S}|\Psi_l\rangle=\omega_l|\varphi_l\rangle, \tag{3}$$

where $|\varphi_l\rangle$ is an eigenvector of the matrix $\mathcal{S}\mathcal{S}^T$ associated with the same eigenvalue ω_l^2.

B. Displacements toward mechanical equilibrium

The first observable we consider is the mean-squared displacements u^2 between the initial network—before the restlength shifts are introduced—and the force-balanced configurations obtained after introducing the restlength shifts and minimizing the energy. Assuming the springs all share the same unit stiffnesses, the net force $|F\rangle$ on the nodes due to introducing the restlength shifts $|\delta\ell\rangle$ can be written as

$$|F\rangle=\mathcal{S}^T|\delta\ell\rangle=w\,\mathcal{S}^T|\eta\rangle, \tag{4}$$

where we have defined $|\delta\ell\rangle=w|\eta\rangle$ and η is a vector of $Nz/2$ uncorrelated, normally distributed random variables with unit variance and zero mean.

The linear displacement response to introducing the restlength shifts is therefore

$$|u\rangle=\mathcal{H}^{-1}|F\rangle=w\mathcal{H}^{-1}\mathcal{S}^T|\eta\rangle, \tag{5}$$

and therefore its square magnitude follows [28]

$$\begin{aligned}u^2&=\langle u|u\rangle=\langle F|\mathcal{H}^{-2}|F\rangle=w^2\langle\eta|\mathcal{S}\mathcal{H}^{-2}\mathcal{S}^T|\eta\rangle\\&=w^2\sum_l\frac{\langle\eta|\mathcal{S}|\Psi_l\rangle\langle\Psi_l|\mathcal{S}^T|\eta\rangle}{\omega_l^4}=w^2\sum_l\frac{\langle\eta|\mathcal{S}|\Psi_l\rangle^2}{\omega_l^4}\\&=w^2\sum_l\frac{\langle\eta|\varphi_l\rangle^2}{\omega_l^2}\sim w^2\int_{\delta z}\frac{D(\omega)d\omega}{\omega^2}\sim\frac{w^2}{\delta z}\sim\delta z\left(\frac{w}{\delta z}\right)^2,\end{aligned} \tag{6}$$

where we have suppressed the trivial $\sim N$ dependence, and used Eq. (3). The above argument implies that, in the linear regime, $u^2/\delta z$ should be a quadratic function of the ratio $w/\delta z$, and that the relevant scale for the restlength shifts in our system is $w_\star\sim\delta z$. Indeed, in the linear-response regime, we expect a ballistic behavior of displacements (where the role of time is played by w), consistent with the above arguments.

Given the above result, we make the scaling ansatz

$$u^2\sim\delta z\,\mathcal{F}_u(w/\delta z), \tag{7}$$

where the scaling function $\mathcal{F}_u(y)$ satisfies $\mathcal{F}_u(y)\sim y^2$ for $y\equiv w/\delta z\ll 1$. Furthermore, since one expects that the nonlinear displacement response should become diffusive, we expect $\mathcal{F}_u(y)\sim y$ for $y\gg 1$.

All the above predictions are validated in Fig. 2; we find that the scaling form Eq. (7) leads to a convincing data collapse. Importantly, we further note that, in the nonlinear (diffusive) regime $w\gg\delta z$, Eq. (7) indicates that $u^2\sim w$, independent of the coordination z. We therefore postulate that, since displacements become coordination independent in the nonlinear regime, then other observables of interest will also show z independence for $w\gg\delta z$. In what follows, we will use this assumption of z independence, together with linear response arguments, to obtain the scaling exponents of various observables in the nonlinear, $w\gg\delta z$ regime.

C. Potential energy

The potential energy U of our model reads

$$U(w)=\sum_{\text{springs }i,\,j}(r_{ij}-\ell_{ij}(w))^2, \tag{8}$$

where the restlengths $\ell_{ij}(w)=\ell_{ij}^{(0)}+\delta\ell_{ij}(w)$ with $\delta\ell_{ij}(w)=w\eta_{ij}$ and η_{ij} are normally distributed, uncorrelated random variables with unit variance and zero mean. In the harmonic regime, the potential energy is obtained by approximating $U(w)\simeq\frac{d^2U}{dw^2}|_{w=0}w^2$, where the total derivatives d/dw are taken under the preservation of mechanical equilibrium [52]. In addition, we recall that since $U(w=0)=0$, together with that the reflection symmetry $w\to-w$ implies that $dU/dw=0$, one deduces the quadratic scaling of the energy with w.

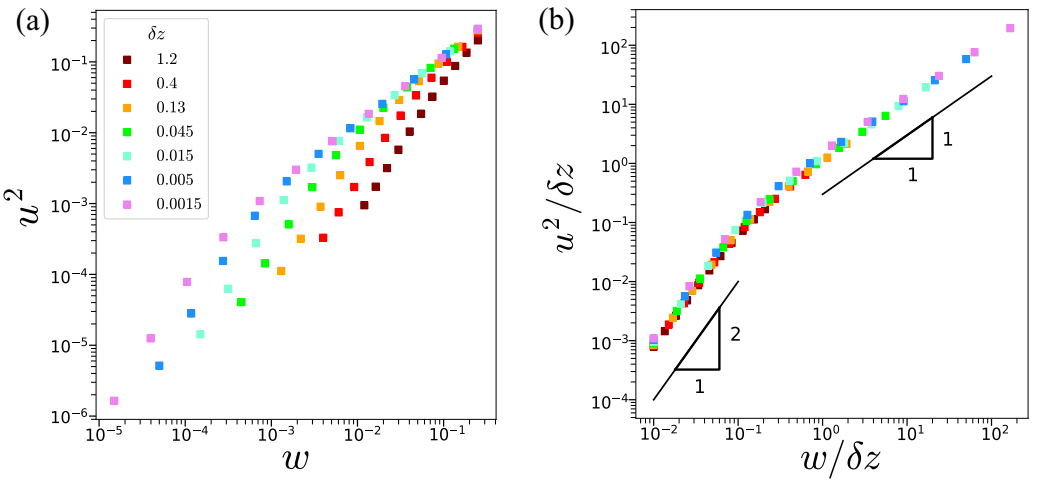

FIG. 2. Mean squared displacements u^2 between the relaxed, initial network, and the network obtain after introducing the mechanical frustration and minimizing the energy, as described in the text. Panel (a) shows the raw data for various coordinations z and widths w (see text for definitions). Panel (b) employs the scaling form of Eq. (7) to find a convincing data collapse, validating the predicted crossover between ballistic and diffusive behavior. This form indicates that, at high w's, observables becomes z independent, see text for discussion.

The second derivative reads [46,48,53]

$$\left.\frac{d^2U}{dw^2}\right|_{w=0} = \langle\eta|\eta\rangle - \langle\eta|\mathcal{S}\mathcal{H}^{-1}\mathcal{S}^T|\eta\rangle$$
$$= \langle\eta|(\mathcal{I} - \mathcal{S}\mathcal{H}^{-1}\mathcal{S}^T)|\eta\rangle \sim N\delta z,$$

and so we expect that, for small w,

$$\frac{U(w)}{N} \sim \delta z\, w^2 \sim \delta z^3\left(\frac{w}{\delta z}\right)^2. \tag{9}$$

The linear response result derived above suggests that the energy per particle is given by the following scaling form:

$$U/N = \delta z^3 \mathcal{F}_U(w/\delta z), \tag{10}$$

where $\mathcal{F}_U(y)\sim y^2$ for $y\ll 1$. As discussed above, if we accept the postulation that observables must become independent of z at large w, then we expect $\mathcal{F}_U(y)\sim y^3$ for $y\gg 1$, or $U/N\sim w^3$ for $w\gg\delta z$. These predictions are validated in Fig. 3.

D. Shear modulus

We next analyze the shear modulus G of our glassy configurations; microscopic expressions are available, e.g., in [52]. In the unjamming literature it is well-known that, for relaxed spring networks at coordination z, $G\sim\delta z$. We thus make the following scaling ansatz:

$$G \sim \delta z\, \mathcal{F}_G(w/\delta z), \tag{11}$$

where $\mathcal{F}_G(y)\to$ const for $y\ll 1$. Demanding once again that G becomes z independent at large w, we predict $G\sim w$ for $w\gg\delta z$, and thus $\mathcal{F}_G(y)\sim y$ for $y\gg 1$. These predictions are validated in Fig. 4.

E. Characteristic mesoscopic elastic stiffness

After having analyzed the macroscopic shear modulus G in the previous subsection, it is interesting to consider how the mesoscopic stiffness associated with local perturbations behaves in our model systems. Interestingly, in Refs. [33,54,55]

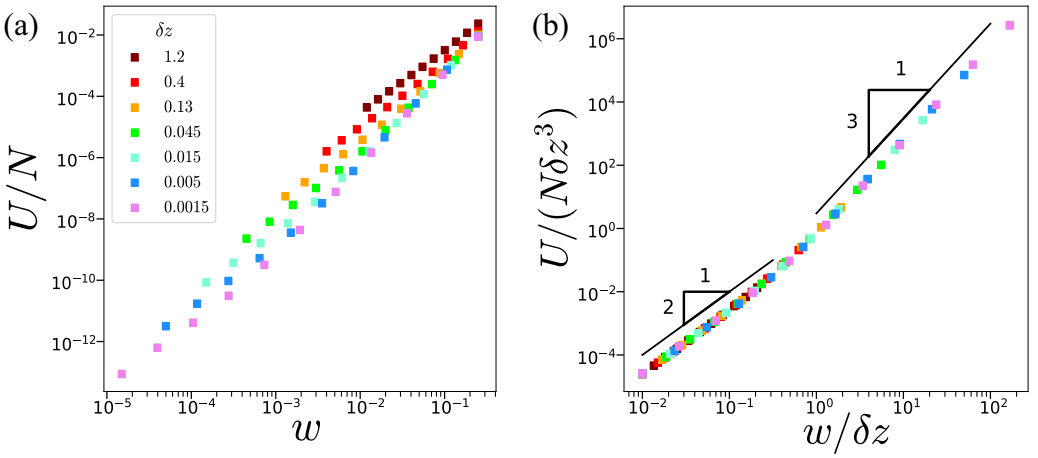

FIG. 3. (a) Potential energy per particle U/N plotted under variations of the width w and various coordinations z as detailed in the legend. (b) The scaling form of Eq. (10) leads to a convincing collapse, see text for further details.

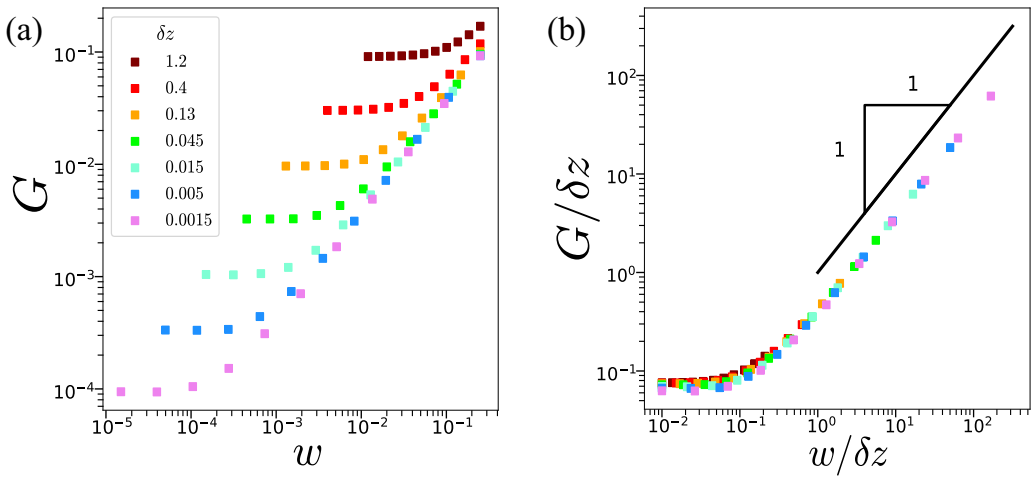

FIG. 4. (a) Shear modulus G plotted under variations of the width w and various coordinations z as detailed in the legend. (b) The scaling form of Eq. (11) leads to a convincing collapse, see text for further details.

it was shown that mesoscopic stiffnesses of the type discussed in what follows are more susceptible to thermal annealing compared to macroscopic elastic moduli, in simple models of computer glasses quenched from a melt. Similar ideas and their implications on supercooled liquids' vibrational entropy and fragility were put forward earlier in Ref. [56]. Finally, in the unjamming literature it has been shown [48,57–59] that the stiffness $\omega_\star^2 \sim \delta z^2$ associated with anomalous vibrational modes in disordered, relaxed spring networks vanishes more quickly upon approaching the unjamming point, compared to the macroscopic shear modulus—which vanishes as δz. These previous results indicate that mesoscopic and macroscopic stiffnesses quite generically feature different dependencies on glass control parameters in several scenarios.

In order to probe the mesoscopic stiffness in our model, we choose a random pair of nodes i, j that are positioned close to each other, but are not connected by a spring. The choice of the pair to pinch was performed extracting a random node i from our network and scanning through its neighboring nodes within a distance smaller than a certain threshold (initially set to 0.9 times the average distance between connected pairs). The first neighboring node found to not be connected to i constitutes the node j of the pair. If no node that fulfils the requirements is found, the threshold is gradually incremented until a disconnected node is found. We then apply a unit force dipole of the form $\boldsymbol{d}_k^{ij} = (\delta_{jk} - \delta_{ik})\boldsymbol{n}_{ij}$ to the selected pair of nodes (here n_{ij} is the unit vector pointing from node i to node j), and obtain the displacement response $\boldsymbol{D}_k^{ij} = \boldsymbol{\mathcal{H}}_{k\ell}^{-1} \cdot \boldsymbol{d}_\ell^{ij}$ to the force dipole. The stiffness κ_{ij} associated with this perturbation is then

$$\kappa_{ij} = \frac{\boldsymbol{D}^{ij} \cdot \boldsymbol{\mathcal{H}} \cdot \boldsymbol{D}^{ij}}{\boldsymbol{D}^{ij} \cdot \boldsymbol{D}^{ij}} = \frac{\boldsymbol{d}^{ij} \cdot \boldsymbol{\mathcal{H}}^{-1} \cdot \boldsymbol{d}^{ij}}{\boldsymbol{d}^{ij} \cdot \boldsymbol{\mathcal{H}}^{-2} \cdot \boldsymbol{d}^{ij}}. \tag{12}$$

In what follows we consider the average $\kappa \equiv \langle \kappa_{ij} \rangle_{ij}$ over a random selection of 5000 disconnected pairs i, j in our ensemble of glassy samples. According to Ref. [46], in relaxed spring networks (i.e., for $w = 0$ in our model) the numerator of Eq. (12) is expected to scale as δz, and according to Refs. [28,59] the denominator of Eq. (12) should scale as $1/\delta z$, leaving us with the prediction $\kappa \sim \delta z^2$ for $w \to 0$, in agreement with the arguments of Ref. [59] for $\omega_\star^2 \sim \delta z^2$.

What happens to the mesoscopic stiffness κ upon introducing mechanical frustration into the network? As done above, we make the scaling ansatz

$$\kappa \sim \delta z^2 \, \mathcal{F}_\kappa(w/\delta z), \tag{13}$$

such that $\mathcal{F}_\kappa(y) \to$ const for $y \ll 1$. Requiring that κ becomes z independent at large w, we predict that $\mathcal{F}_\kappa(y) \sim y^2$, and so we expect that $\kappa \sim w^2$ at large w. This result should be compared (in the context of the discussion above) with $G \sim w$ in the same, nonlinear regime, indicating that the relation $\kappa \sim G^2$ holds both in the linear and nonlinear regimes. A similar universality was recently pointed out in Ref. [60] for spring networks endowed with weak bending interactions. Our predictions are verified in Fig. 5.

F. Mechanical disorder

We end this Section with the behavior of the dimensionless quantifier χ of mechanical disorder, defined as [5,16,26,61,62]

$$\chi \equiv \sqrt{N} \frac{\text{std(G)}}{\text{mean}(G)}, \tag{14}$$

where std(•) stands for the ensemble standard deviation, and mean(•) refers to the ensemble mean. The $\sqrt{N}$ factor ensures χ is N independent (for large-enough N). In previous work it has been shown that for relaxed spring networks with coordination z, $\chi \sim 1/\sqrt{\delta z}$ [16,62]. We therefore make the scaling ansatz that

$$\chi \sim \delta z^{-1/2} \, \mathcal{F}_\chi(w/\delta z), \tag{15}$$

where $\mathcal{F}_\chi(y) \to$ const for small y. Requiring that χ becomes z independent at large w implies $\chi \sim 1/\sqrt{w}$ at large w, and so $\mathcal{F}_\chi(y) \sim y^{-1/2}$ for $y \gg 1$. All these predictions are validated in Fig. 6. We note that, for estimating std(G) we employed that outlier elimination method presented and explained in Ref. [26].

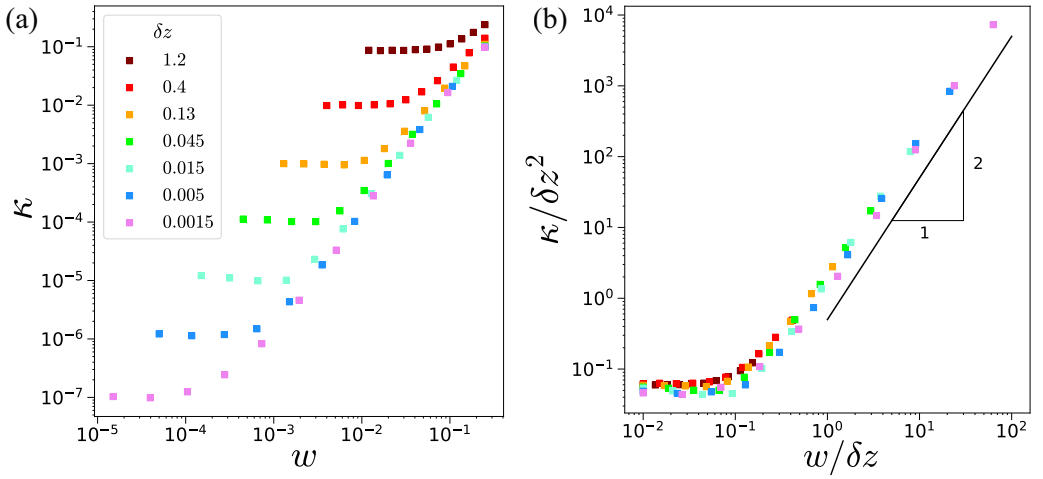

FIG. 5. (a) Mesoscopic elastic stiffness κ plotted under variations of the amplitude of the restlength noise w and various coordinations z as detailed in the legend. (b) The scaling form of Eq. (13) leads to a convincing collapse, see text for further details.

IV. SUMMARY, DISCUSSION, AND OUTLOOK

In this work we have studied and rationalized the elastic properties of a minimal model for the elasticity of glassy solids in which the degree of mechanical disorder can be tuned over a large range, cf. Fig. 6(a). At the same time, and different from some other models for glass elasticity, this minimal model features the universal $\sim\omega^4$ nonphononic spectrum (cf. Fig. 1), which implies that it can better represent more realistic glassy solids compared to other computational models in which mechanical disorder is tunable [5,16,24,27,28]. Our approach is the same as one of the recently introduced schemes of Ref. [44] where the floppy regime and spring-pruning effects were studied. It also bears similarity to the approach taken in Ref. [6], however, there the interplay between coordination and mechanical frustration was not considered. Finally, our work also echoes the approaches of Refs. [27,63], in which mechanical frustration is incorporated into a theory for glass elasticity, however these approaches do not predict the existence of quasilocalized modes nor the quartic nonphononic spectrum observed in computer glasses.

The model studied here—a mechanically frustrated bead-spring network—features a transition from a coordination-dependent regime, to a coordination-independent regime, at a characteristic mechanical frustration scale $w_\star \sim \delta z$. This transition can be understood by considering the displacements of the nodes upon introducing mechanical frustration into the network. Then, combining the expected diffusive behavior of the networks' nodes for high frustration w—with the ballistic behavior seen in the linear response analysis at low w gives rise to the characteristic scale $w_\star \sim \delta z$ for the transition between the two regimes, cf. Sec. III B. The connectivity independence found for the mean squared displacement above the characteristic scale $w_\star$ was postulated to hold for any observable $\mathcal{O}$, and allowed us to obtain a family of scaling functions $\mathcal{F}_\mathcal{O}(w/\delta z)$ and their associated scaling exponents, which completely describe the behavior of the observables in both regimes, and were all convincingly validated by numerical simulations.

In Refs. [37,38] a mean-field model of coupled anharmonic oscillators was formulated and analyzed; that model's

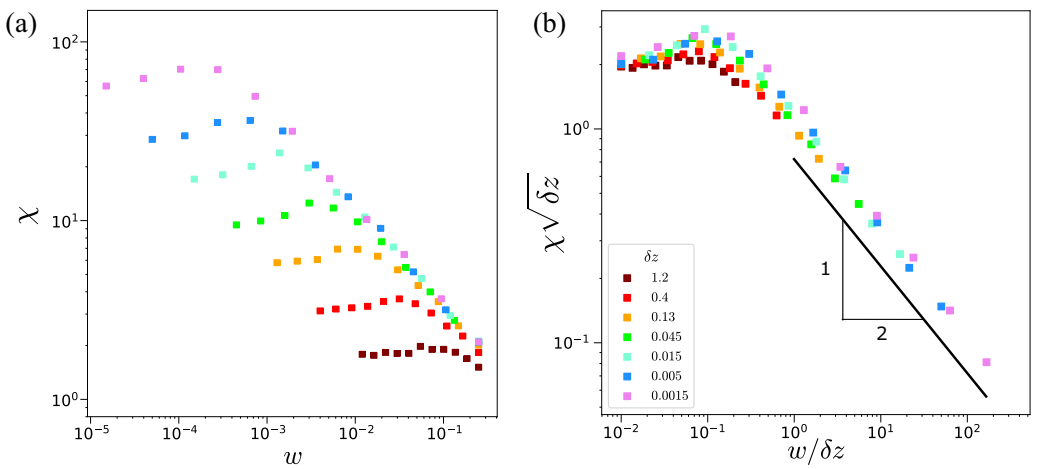

FIG. 6. (a) Dimensionless mechanical disorder quantifier χ plotted under variations of the amplitude of the restlength noise w and various coordinations z as detailed in the legend. (b) The scaling form of Eq. (15) leads to a convincing collapse, see text for further details.

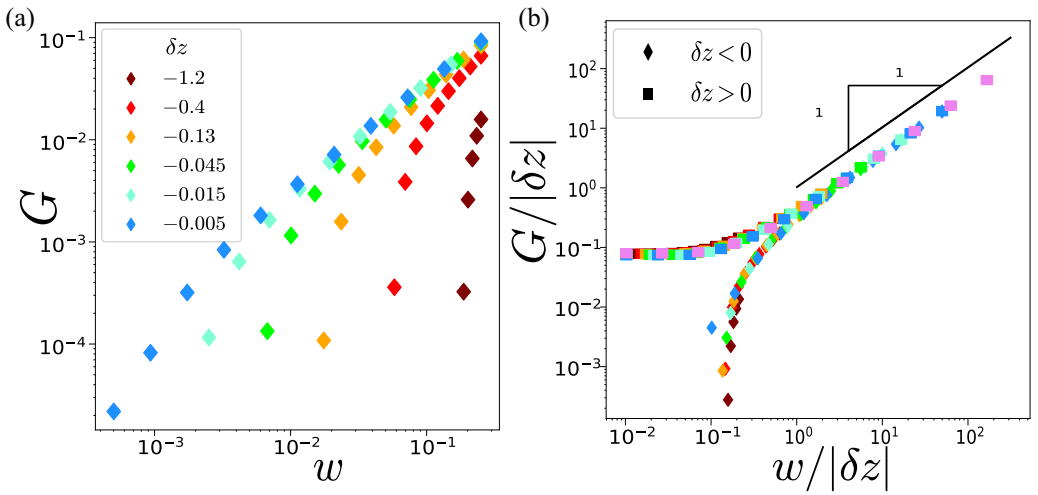

FIG. 7. (a) The shear modulus G of hypostatic networks with $z < z_c \equiv 2d$ and $N = 16\,000$, shown here for various degrees of mechanical frustration w. In this case, each datapoint is obtained by averaging over 2500 independently built networks. (b) The same scaling form Eq. (11) for the shear modulus of hyperstatic networks with $z > z_c$–also collapses the shear modulus of frustrated hypostatic networks, and reveals the characteristic frustration scale $w_\star \sim |\delta z|$ above which G becomes finite, reminiscent of the characteristic stiffening strain scale $\gamma_\star$ above which deformed floppy networks acquire a finite shear modulus, see text for further discussion.

vibrational spectrum reproduces two features also seen in the nonphononic spectra of computer glasses: (i) it follows $\mathcal{D}(\omega) = A_g \omega^4$ in many regions of the model's parameter space, and (ii) the prefactor A_g is exponentially suppressed as a function of the relevant combination of the model's parameters, akin to the Boltzmann-like reduction seen in A_g of deeply supercooled computer glasses [33,64]—with the (equilibrium) parent temperature T_p from which glassy samples were (instantaneously) quenched playing the role of the equilibrium temperature in the Boltzmann-like relation. In future work we plan to investigate how the prefactor $A_g(z, w)$ behaves as a function of the coordination z and the mechanical frustration w in our minimal model—to the aim of constructing a mapping between the parameters of the aforementioned mean-field model, and the degree of frustration or proximity to unjamming in finite-dimensional computer glass models. Such a mapping might help shed light on the origin of the universal quartic nonphononic spectra seen in many computer glass models.

Finally, we note that the characteristic mechanical-frustration scale $w_\star \sim \delta z$ (cf. discussion in Sec. III B) is reminiscent of the scaling $\gamma_\star \sim |\delta z|$ of the stiffening strain $\gamma_\star$ at which floppy, disordered spring networks—featuring $z < z_c$—acquire a finite shear modulus upon subjection to spatial deformations [40,41,65,66]. Indeed, and as shown in Ref. [44], a floppy network with a vanishing shear modulus $G = 0$ can be made rigid and acquire a finite shear modulus by introducing mechanical frustration—in the form of noise in the network's springs' restlengths, as done here. Similarly, in Ref. [67] it was shown how motor-generated stresses can rigidify floppy elastic networks.

We demonstrate this effect in Fig. 7, where the shear modulus of floppy networks with $z < z_c$ is plotted vs w for a variety of coordinations as detailed by the figure legend. Different from strain stiffening, in this case our frustrated floppy networks with $w < |\delta z|$ can carry a finite (though small) elastic energy $U/N > 0$, but—at the same time—also have a vanishing shear modulus $G = 0$, while strained floppy networks below the stiffening strain—i.e., with $\gamma < \gamma_\star \sim |\delta z|$—have a vanishing shear modulus $G = 0$ but also carry no elastic energy, i.e., $U/N = 0$. Interestingly, the same scaling variable $w/|\delta z|$—put forward and motivated for systems above the jamming point with $z > z_c$—collapses the $z < z_c$ data as well, as shown in Fig. 7(b), in which we also included the hyperstatic ($z > z_c$) data set. In future work we plan to investigate how the vibrational density of states of hypostatic samples that were rigidified (i.e., acquire a finite shear modulus $G > 0$) by frustration—behaves as compared to hyperstatic frustrated networks.

ACKNOWLEDGMENTS

We thank Eran Bouchbinder and Joshua Dijksman for invaluable discussions. This work was supported by the Institute of Physics of the University of Amsterdam. G.D. acknowledges support from Fondecyt Grant No. 1210656.

[1] W. Schirmacher, G. Ruocco, and T. Scopigno, Acoustic attenuation in glasses and its relation with the boson peak, Phys. Rev. Lett. **98**, 025501 (2007).

[2] A. Marruzzo, W. Schirmacher, A. Fratalocchi, and G. Ruocco, Heterogeneous shear elasticity of glasses: The origin of the boson peak, Sci. Rep. **3**, 1407 (2013).

[3] A. Moriel, G. Kapteijns, C. Rainone, J. Zylberg, E. Lerner, and E. Bouchbinder, Wave attenuation in glasses: Rayleigh and generalized-rayleigh scattering scaling, J. Chem. Phys. **151**, 104503 (2019).

[4] L. Wang, G. Szamel, and E. Flenner, Sound attenuation in finite-temperature stable glasses, Soft Matter **16**, 7165 (2020).

[5] G. Kapteijns, D. Richard, E. Bouchbinder, and E. Lerner, Elastic moduli fluctuations predict wave attenuation rates in glasses, J. Chem. Phys. **154**, 081101 (2021).
[6] S. Mahajan and M. P. Ciamarra, Quasi-localized vibrational modes, boson peak and sound attenuation in model mass-spring networks, SciPost Phys. **15**, 069 (2023).
[7] Y. Shi and M. L. Falk, Strain localization and percolation of stable structure in amorphous solids, Phys. Rev. Lett. **95**, 095502 (2005).
[8] E. Bouchbinder and J. S. Langer, Nonequilibrium thermodynamics of driven amorphous materials. III. Shear-transformation-zone plasticity, Phys. Rev. E **80**, 031133 (2009).
[9] M. Ozawa, L. Berthier, G. Biroli, A. Rosso, and G. Tarjus, Random critical point separates brittle and ductile yielding transitions in amorphous materials, Proc. Natl. Acad. Sci. USA **115**, 6656 (2018).
[10] Y. Jin, P. Urbani, F. Zamponi, and H. Yoshino, A stability-reversibility map unifies elasticity, plasticity, yielding, and jamming in hard sphere glasses, Sci. Adv. **4**, eaat6387 (2018).
[11] C. H. Rycroft and E. Bouchbinder, Fracture toughness of metallic glasses: Annealing-induced embrittlement, Phys. Rev. Lett. **109**, 194301 (2012).
[12] J. Ketkaew, W. Chen, H. Wang, A. Datye, M. Fan, G. Pereira, U. D. Schwarz, Z. Liu, R. Yamada, W. Dmowski, M. D. Shattuck, C. S. O'Hern, T. Egami, E. Bouchbinder, and J. Schroers, Mechanical glass transition revealed by the fracture toughness of metallic glasses, Nat. Commun. **9**, 3271 (2018).
[13] D. Richard, E. Lerner, and E. Bouchbinder, Brittle-to-ductile transitions in glasses: Roles of soft defects and loading geometry, MRS Bull. **46**, 902 (2021).
[14] S. Patinet, D. Vandembroucq, and M. L. Falk, Connecting local yield stresses with plastic activity in amorphous solids, Phys. Rev. Lett. **117**, 045501 (2016).
[15] D. Richard, M. Ozawa, S. Patinet, E. Stanifer, B. Shang, S. A. Ridout, B. Xu, G. Zhang, P. K. Morse, J.-L. Barrat, L. Berthier, M. L. Falk, P. Guan, A. J. Liu, K. Martens, S. Sastry, D. Vandembroucq, E. Lerner, and M. L. Manning, Predicting plasticity in disordered solids from structural indicators, Phys. Rev. Mater. **4**, 113609 (2020).
[16] K. González-López, E. Bouchbinder, and E. Lerner, Variability of mesoscopic mechanical disorder in disordered solids, J. Non-Cryst. Solids **604**, 122137 (2023).
[17] G. Jung, R. M. Alkemade, V. Bapst, D. Coslovich, L. Filion, F. P. Landes, A. Liu, F. S. Pezzicoli, H. Shiba, G. Volpe *et al.*, Roadmap on machine learning glassy liquids, arXiv:2311.14752.
[18] D. Richard, Connecting microscopic and mesoscopic mechanics in model structural glasses, arXiv:2311.09917.
[19] C. P. Royall and S. R. Williams, The role of local structure in dynamical arrest, Phys. Rep. **560**, 1 (2015).
[20] H. Tong and H. Tanaka, Structural order as a genuine control parameter of dynamics in simple glass formers, Nat. Commun. **10**, 5596 (2019).
[21] E. Bouchbinder and J. Langer, Nonequilibrium thermodynamics of driven amorphous materials. II. Effective-temperature theory, Phys. Rev. E **80**, 031132 (2009).
[22] C. Brito, E. Lerner, and M. Wyart, Theory for swap acceleration near the glass and jamming transitions for continuously polydisperse particles, Phys. Rev. X **8**, 031050 (2018).
[23] G. Kapteijns, W. Ji, C. Brito, M. Wyart, and E. Lerner, Fast generation of ultrastable computer glasses by minimization of an augmented potential energy, Phys. Rev. E **99**, 012106 (2019).
[24] E. Lerner and E. Bouchbinder, Frustration-induced internal stresses are responsible for quasilocalized modes in structural glasses, Phys. Rev. E **97**, 032140 (2018).
[25] A. Ninarello, L. Berthier, and D. Coslovich, Models and algorithms for the next generation of glass transition studies, Phys. Rev. X **7**, 021039 (2017).
[26] G. Kapteijns, E. Bouchbinder, and E. Lerner, Unified quantifier of mechanical disorder in solids, Phys. Rev. E **104**, 035001 (2021).
[27] E. DeGiuli, A. Laversanne-Finot, G. During, E. Lerner, and M. Wyart, Effects of coordination and pressure on sound attenuation, boson peak and elasticity in amorphous solids, Soft Matter **10**, 5628 (2014).
[28] E. Lerner, E. DeGiuli, G. During, and M. Wyart, Breakdown of continuum elasticity in amorphous solids, Soft Matter **10**, 5085 (2014).
[29] V. Karpov and D. Parshin, On the thermal conductivity of glasses at temperatures below the debye temperature, Zh. Eksp. Teor. Fiz. **88**, 2212 (1985).
[30] M. Ilyin, V. Karpov, and D. Parshin, Parameters of soft atomic potentials in glasses, Zh. Eksp. Teor. Fiz. **92**, 291 (1987).
[31] E. Lerner and E. Bouchbinder, Low-energy quasilocalized excitations in structural glasses, J. Chem. Phys. **155**, 200901 (2021).
[32] L. Wang, A. Ninarello, P. Guan, L. Berthier, G. Szamel, and E. Flenner, Low-frequency vibrational modes of stable glasses, Nat. Commun. **10**, 26 (2019).
[33] C. Rainone, E. Bouchbinder, and E. Lerner, Pinching a glass reveals key properties of its soft spots, Proc. Natl. Acad. Sci. USA **117**, 5228 (2020).
[34] Discussions about glass-formation-protocol-induced finite-size effects in the nonphononic spectrum of computer glasses can be found in Refs. [68–72].
[35] G. Kapteijns, E. Bouchbinder, and E. Lerner, Universal nonphononic density of states in 2D, 3D, and 4D glasses, Phys. Rev. Lett. **121**, 055501 (2018).
[36] D. Richard, K. González-López, G. Kapteijns, R. Pater, T. Vaknin, E. Bouchbinder, and E. Lerner, Universality of the nonphononic vibrational spectrum across different classes of computer glasses, Phys. Rev. Lett. **125**, 085502 (2020).
[37] C. Rainone, P. Urbani, F. Zamponi, E. Lerner, and E. Bouchbinder, Mean-field model of interacting quasilocalized excitations in glasses, SciPost Phys. Core **4**, 008 (2021).
[38] E. Bouchbinder, E. Lerner, C. Rainone, P. Urbani, and F. Zamponi, Low-frequency vibrational spectrum of mean-field disordered systems, Phys. Rev. B **103**, 174202 (2021).
[39] A. Sharma, A. J. Licup, K. A. Jansen, R. Rens, M. Sheinman, G. H. Koenderink, and F. C. MacKintosh, Strain-controlled criticality governs the nonlinear mechanics of fibre networks, Nat. Phys. **12**, 584 (2016).
[40] R. Rens, C. Villarroel, G. Düring, and E. Lerner, Micromechanical theory of strain stiffening of biopolymer networks, Phys. Rev. E **98**, 062411 (2018).
[41] E. Lerner and E. Bouchbinder, Scaling theory of critical strain-stiffening in disordered elastic networks, Extreme Mech. Lett. **65**, 102104 (2023).
[42] E. Lerner and E. Bouchbinder, Anomalous linear elasticity of disordered networks, Soft Matter **19**, 1076 (2023).

[43] E. Bitzek, P. Koskinen, F. Gähler, M. Moseler, and P. Gumbsch, Structural relaxation made simple, Phys. Rev. Lett. **97**, 170201 (2006).
[44] M. A. G. Cunha, J. C. Crocker, and A. J. Liu, Building rigid networks with prestress and selective pruning, arXiv:2312.06119.
[45] E. Lerner, G. Düring, and M. Wyart, A unified framework for non-brownian suspension flows and soft amorphous solids, Proc. Natl. Acad. Sci. USA **109**, 4798 (2012).
[46] E. Lerner, Quasilocalized states of self stress in packing-derived networks, Eur. Phys. J. E **41**, 93 (2018).
[47] C. R. Calladine, Buckminster Fuller's Tensegrity structures and Clerk Maxwell's rules for the construction of stiff frames, Int. J. Solids Struct. **14**, 161 (1978).
[48] M. Wyart, On the rigidity of amorphous solids, Ann. Phys. Fr. **30**, 1 (2005).
[49] G. Düring, E. Lerner, and M. Wyart, Phonon gap and localization lengths in floppy materials, Soft Matter **9**, 146 (2013).
[50] Y. M. Beltukov, Random matrix theory approach to vibrations near the jamming transition, JETP Lett. **101**, 345 (2015).
[51] H. Mizuno, K. Saitoh, and L. E. Silbert, Elastic moduli and vibrational modes in jammed particulate packings, Phys. Rev. E **93**, 062905 (2016).
[52] J. F. Lutsko, Generalized expressions for the calculation of elastic constants by computer simulation, J. Appl. Phys. **65**, 2991 (1989).
[53] W. G. Ellenbroek, Z. Zeravcic, W. van Saarloos, and M. van Hecke, Non-affine response: Jammed packings vs. spring networks, Europhys. Lett. **87**, 34004 (2009).
[54] E. Lerner and E. Bouchbinder, A characteristic energy scale in glasses, J. Chem. Phys. **148**, 214502 (2018).
[55] K. González-López, M. Shivam, Y. Zheng, M. P. Ciamarra, and E. Lerner, Mechanical disorder of sticky-sphere glasses. II. thermomechanical inannealability, Phys. Rev. E **103**, 022606 (2021).
[56] M. Wyart, Correlations between vibrational entropy and dynamics in liquids, Phys. Rev. Lett. **104**, 095901 (2010).
[57] M. Wyart, L. E. Silbert, S. R. Nagel, and T. A. Witten, Effects of compression on the vibrational modes of marginally jammed solids, Phys. Rev. E **72**, 051306 (2005).
[58] M. Wyart, Scaling of phononic transport with connectivity in amorphous solids, Europhys. Lett. **89**, 64001 (2010).
[59] L. Yan, E. DeGiuli, and M. Wyart, On variational arguments for vibrational modes near jamming, Europhys. Lett. **114**, 26003 (2016).
[60] E. Lerner, Effects of coordination and stiffness scale-separation in disordered elastic networks, arXiv:2312.06427.
[61] E. Bouchbinder and E. Lerner, Universal disorder-induced broadening of phonon bands: From disordered lattices to glasses, New J. Phys. **20**, 073022 (2018).
[62] J. A. Giannini, E. Lerner, F. Zamponi, and M. L. Manning, Scaling regimes and fluctuations of observables in computer glasses approaching the unjamming transition, J. Chem. Phys. **160**, 034502 (2024).
[63] M. Shimada and E. D. Giuli, Random quench predicts universal properties of amorphous solids, SciPost Phys. **12**, 090 (2022).
[64] W. Ji, T. W. J. de Geus, M. Popović, E. Agoritsas, and M. Wyart, Thermal origin of quasilocalized excitations in glasses, Phys. Rev. E **102**, 062110 (2020).
[65] M. Wyart, H. Liang, A. Kabla, and L. Mahadevan, Elasticity of floppy and stiff random networks, Phys. Rev. Lett. **101**, 215501 (2008).
[66] G. Düring, E. Lerner, and M. Wyart, Length scales and self-organization in dense suspension flows, Phys. Rev. E **89**, 022305 (2014).
[67] M. Sheinman, C. P. Broedersz, and F. C. MacKintosh, Actively stressed marginal networks, Phys. Rev. Lett. **109**, 238101 (2012).
[68] E. Lerner, Finite-size effects in the nonphononic density of states in computer glasses, Phys. Rev. E **101**, 032120 (2020).
[69] L. Wang, G. Szamel, and E. Flenner, Erratum: Low-frequency excess vibrational modes in two-dimensional glasses [Phys. Rev. Lett. 127, 248001 (2021)], Phys. Rev. Lett. **129**, 019901 (2022).
[70] E. Lerner and E. Bouchbinder, Nonphononic spectrum of two-dimensional structural glasses, J. Chem. Phys. **157**, 166101 (2022).
[71] L. Wang, L. Fu, and Y. Nie, Density of states below the first sound mode in 3D glasses, J. Chem. Phys. **157**, 074502 (2022).
[72] L. Wang, G. Szamel, and E. Flenner, Scaling of the nonphononic spectrum of two-dimensional glasses, J. Chem. Phys. **158**, 126101 (2023).